

Slow light of an amplitude modulated Gaussian pulse in electromagnetically induced transparency medium

Wenzhuo Tang, Bin Luo, Yu Liu, and Hong Guo*

*CREAM Group, State Key Laboratory of Advanced Optical Communication Systems and Networks (Peking University)
and Institute of Quantum Electronics, School of Electronics Engineering and Computer Science (EECS),*

Peking University, Beijing 100871, China

**Corresponding author: hongguo@pku.edu.cn*

Compiled October 26, 2021

The slow light effects of an amplitude modulated Gaussian (AMG) pulse in a cesium atomic vapor cell are presented. In a single- Λ type electromagnetically induced transparency (EIT) medium, more severe distortion is observed for the AMG pulse than a Gaussian one. Using Fourier spectrum analysis, we find that it is the linear absorption of the medium that mainly causes the loss and distortion of the slowed pulse. Further, it is found that the dispersion determines the group velocities and causes an additional distortion of the AMG pulse due to its spectral distribution. Based on the transmission (absorption) spectrum, we propose a post-processing method to recover the shape and intensity of the slowed pulse. In addition, this method reveals a novel way to obtain the simultaneously slow and fast light of different spectral components of a single pulse. © 2021 Optical Society of America

OCIS codes: 270.1670, 270.5530.

1. INTRODUCTION

Recently, slow light has attracted tremendous attention for its potential applications in optical communication. Group velocity of an optical pulse can be slowed down using various effects, such as electromagnetically induced transparency (EIT) [1,2], double absorption line [3,4], coherent population oscillations [5,6], stimulated Brillouin scattering [7] and stimulated Raman scattering [8], etc. EIT is the most popular one among these effects, and the pulses used in the slow light experiments are usually of Gaussian shape. Non-Gaussian pulses such as rectangularly and step-modulated Gaussian pulses are also studied in [9,10]. As we know, in real communication, a modulation to the optical pulse is extremely important. However, these studies are based on the shaping of pulse, while the modulation of a single pulse such as cosine type AMG pulse has not been well investigated yet. In this paper, we experimentally demonstrate the slow light effects of an AMG pulse in cesium atomic vapor, and analyze the significant loss and distortion of the AMG pulse due to absorption and dispersion. Further more, a post-processing method is proposed and a well-recovered AMG pulse is obtained. In addition, simultaneously slow and fast light effect of different spectral components of this AMG pulse is observed.

2. SLOW LIGHT EXPERIMENT

Our experimental setup is schematically illustrated in Fig. 1(a). An 852 nm narrowband (~ 300 kHz) diode laser (output power ~ 30 mW) is stabilized to the D_2 transition of ^{133}Cs atom: $F = 3 \rightarrow F' = 2, 4$ crossover. By the combination of $\lambda/2$ (half-wave plate) and PBS1, the laser is divided into two beams, the coupling and the probe, with perpendicular polarizations and adjustable

proportions. The frequency of coupling laser is redshifted ~ 175 MHz by AOM2, with the power ~ 2.35 mW and $1/e^2$ beam diameter ~ 2.0 mm. The probe pulse is generated by passing a weak (< 10 μW) continuous-wave laser through AOM1, with the frequency redshifted ~ 175 MHz and $1/e^2$ beam diameter ~ 2.0 mm. The amplitude of probe field $E(t)$ (nonnegative for convenience in data processing) is proportional to the amplitude of the driving radio-frequency wave to AOM1, which is directly controlled by an arbitrary waveform generator (AWG). After that, both the coupling (vertically polarized) and the probe (horizontally polarized) lasers are resonant with the D_2 transition $F = 3 \rightarrow F' = 2$ of ^{133}Cs atom [see Fig. 1(b)], and combined at PBS2. Then, the two overlapped lasers copropagate through the cell in order to reduce the total Doppler broadening [11]. The beam splitter (BS) in front of the cell splits an appropriate portion of the probe to PD1 as reference, whose intensity is set to be equal to that of the output when the probe is detuned far off-resonant from all atomic transitions. Thus, the background absorption is eliminated and the reference can be treated as “input” in the following analysis. A 10 cm-long paraffin-coated cesium (^{133}Cs) vapor cell at room temperature (~ 25 $^\circ\text{C}$) is placed in the magnetic shield (MS) to screen out the earth magnetic field in lab. The exiting beams are separated by PBS3, so only the slowed probe pulse beam reaches PD2 as the “output” in the following analysis.

In experiment, both the optical intensities $I(t)$ of the reference (treated as “input”) and output pulses are recorded on a 100 MHz digital oscilloscope triggered by the AWG. Thus, the amplitudes of both input and output (slowed) pulses can be obtained from this relation: $E(t) = \sqrt{I(t)}$, which is the reason of requiring the amplitudes of optical pulses to be nonnegative in experiment.

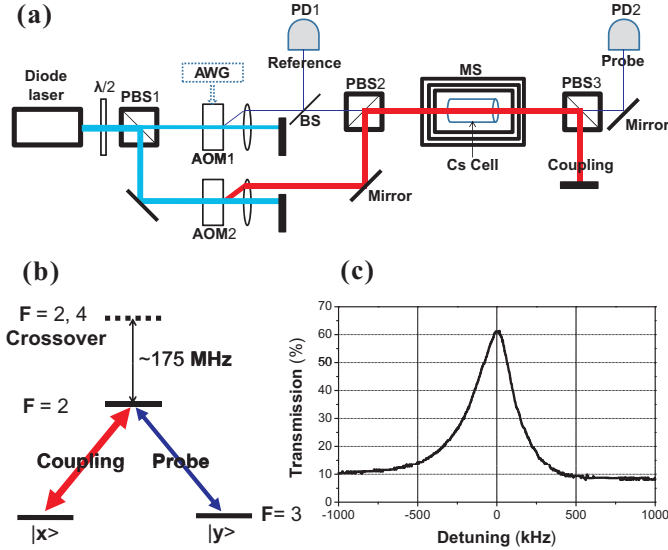


Fig. 1. (color online). (a) Experimental setup. $\lambda/2$, half-wave plate; PBS, polarizing beam splitter; AOM, acousto-optic modulator; AWG, arbitrary waveform generator; MS, magnetic shield; APD, 1 GHz avalanche photo diode. (b) A simplified single- Λ type system of ^{133}Cs atom interacts with the coupling and the probe lasers. Two ground states $|x\rangle$ and $|y\rangle$ represent appropriate superpositions of magnetic sublevels. (c) Probe transmission spectrum (an average of 16 measured results) versus detuning from resonance, with the FWHM bandwidth of ~ 350 kHz and the maximum of $\sim 61.5\%$.

The intensities of two probe (input) pulses in time domain are chosen as

$$\begin{aligned} \text{Gaussian : } I_1(t) &= |E_1(t)|^2 = \exp\left[-\frac{(\ln 2)t^2}{T_0^2}\right], \\ \text{AMG : } I_2(t) &= |E_2(t)|^2 = |E_1(t) \cdot [1 + \cos(2\pi\delta t)]|^2 \\ &= \exp\left[-\frac{(\ln 2)t^2}{T_0^2}\right] \cdot [1 + \cos(2\pi\delta t)]^2, \end{aligned}$$

where $I_1(t)$ and $I_2(t)$ are the intensities of two pulses, respectively; $\delta = 700$ kHz is the modulation frequency, and T_0 is the temporal FWHM duration of the intensity of the Gaussian pulse.

Experimental results are shown in Fig. 2. The Gaussian and cosine-type AMG pulses exhibit quite different slow light effects. In the Gaussian case, the pulse [Fig. 2(a)] is delayed by $\sim 0.47 \mu\text{s}$, with relatively low loss and little pulse distortion. Hence, we can compensate for the loss by directly amplifying the intensity of the pulse with a constant magnitude determined by the system. However, in the AMG case [Fig. 2(b)], the output pulse undergoes relatively high loss and significant distortion, meanwhile the delay time ($\sim 0.14 \mu\text{s}$) is obviously decreased. Thus, the direct amplification is not feasible any more [see the “rescaled” pulse in Fig. 2(b)].

3. DISTORTION DUE TO ABSORPTION AND DISPERSION

It is known that the pulse distortion is caused by both absorption and dispersion [12]. Firstly we analyze the “absorptive distortion” using the transmission spectrum [see Fig. 1(c)]. The intensity spectrums of input and output pulses are calculated out using discrete Fourier transform (DFT) based on experimental results. The compensated spectrum is obtained by output together with transmission spectrum [Fig. 3], and is used to recover the intensity and shape of the slowed pulse. It can be seen that the intensity spectrum of the Gaussian pulse keeps unchanged with the FWHM bandwidth of ~ 74.4 kHz; by contrast, the intensity spectrum of the AMG pulse has *not only* a resonant Gaussian component, but *also* two non-resonant Gaussian sidebands with ± 700 kHz detunings symmetrically. Since the amplitudes of the optical field $E(t)$ and the spectrum $E(\Delta)$ satisfy the Fourier transform relation, this effect can be analyzed through the Fourier intensity spectrums of the two input pulses:

$$\begin{aligned} \text{Gaussian : } I_1(\Delta) &= |E_1(\Delta)|^2 = \exp\left[-\frac{(\ln 2)\Delta^2}{\Omega_0^2}\right], \\ \text{AMG : } I_2(\Delta) &= |E_2(\Delta)|^2 \\ &= I_1(\Delta) + \frac{1}{4}[I_1(\Delta - \delta) + I_1(\Delta + \delta)], \end{aligned}$$

where $I_1(\Delta)$ and $I_2(\Delta)$ are the intensity spectrums of two pulses, respectively; Δ is the probe detuning; Ω_0 (determined by T_0) is the FWHM bandwidth of the intensity spectrum of the Gaussian pulse. From the spectrum $[I_2(\Delta)]$ of the AMG pulse, we can see that the “oscillation” of intensity in time domain $[I_2(t)]$ is due to the interference of its three spectral components: $I_1(\Delta)$, $I_1(\Delta - \delta)$, and $I_1(\Delta + \delta)$.

In an ideal EIT medium, when the coupling field (Ω) keeps unchanged both temporally and spatially, the frequency response function of the slow light system can be expressed as $H(\Delta) = \exp[-\Delta Z / (\Delta - i\Gamma_{EIT})]$, where $\Gamma_{EIT} = |\Omega|^2 / \gamma$ (proportional to the intensity of coupling light) is the bandwidth of EIT profile, Z (proportional to the atomic number and cell length) is the normalized propagation length, and Δ is the detuning of spectral component. Suppose the EIT slow-light system is linear, we have

$$\begin{aligned} E_{out}(\Delta) &= H(\Delta) \cdot E_{in}(\Delta) \\ &= \exp\left[\frac{-\Delta Z}{\Delta - i\Gamma_{EIT}}\right] \cdot E_{in}(\Delta) \\ &= \exp\left[\frac{-\Delta^2 \gamma^2 Z}{\Delta^2 \gamma^2 + |\Omega|^4}\right] \exp\left[\frac{-i\Delta \gamma Z |\Omega|^2}{\Delta^2 \gamma^2 + |\Omega|^4}\right] \cdot E_{in}(\Delta) \\ &\equiv A(\Delta) \cdot e^{-i\Phi(\Delta)} \cdot E_{in}(\Delta), \end{aligned}$$

where $E_{in}(\Delta)[E_{out}(\Delta)]$ represents the amplitude spectrum of the input (output) pulse. Real functions $A(\Delta) \equiv \exp[-\Delta^2 \gamma^2 Z / (\Delta^2 \gamma^2 + \Omega^4)]$ [corresponds to the measured transmission spectrum in Fig. 1(c)] and $\Phi(\Delta) \equiv$

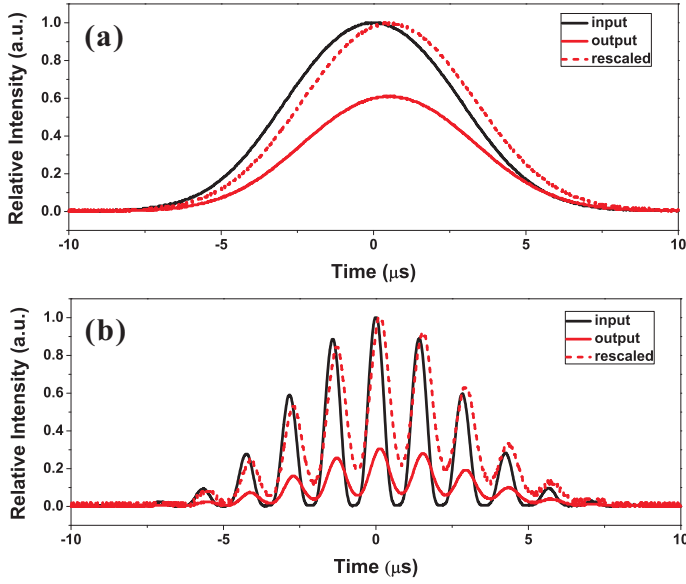


Fig. 2. (color online). Input (normalized) and output pulses in time domain, each pulse is an average of 16 measured results; rescaled is the normalization of output. Pulse delay time $\sim 0.47 \mu\text{s}$ is measured according to the peak of the pulse. (a) Slow light of Gaussian pulse with low loss and little distortion. (b) Slow light of AMG pulse with high loss and significant distortion. Pulse delay time $\sim 0.14 \mu\text{s}$ is measured according to the highest peak of pulse.

$\Delta\gamma Z|\Omega|^2/(\Delta^2\gamma^2+|\Omega|^4)$ are related to the absorption and dispersion, respectively.

Note that, we have $I_{out}(\Delta) = |A(\Delta)|^2 \cdot I_{in}(\Delta)$, where the phase information is eliminated, and $|A(\Delta)|^2$ is the transmission spectrum of the system [see Fig. 1(c)]. Three spectral components experience different transmission rates according to detuning Δ . In the AMG case, two sideband components of the pulse undergo much more severe absorptions than the resonant one. A compensation method is thus applied to recover the output slowed pulse. As shown in Fig. 3, we obtain the compensated spectrums by simply amplifying the output spectrums according to the transmission spectrum, i.e., $I_{comp}(\Delta) = I_{out}(\Delta)/|A(\Delta)|^2_{measured}$. As the compensated and the input spectrums are well overlapped in Fig. 3, this compensation method can *recover* the pulse with high fidelity in shape and intensity. At this point, we can see that it is the frequency dependent absorption that mainly causes the loss and thus the distortion of the pulse. This explanation is more intuitive than “the pulses ‘forget’ their initial temporal shapes”, as stated in [13].

It should be mentioned that, the noise is not considered in this paper for its limited influence. To further confirm this, we transform the compensated spectrum back to time domain using inverse discrete Fourier transform (IDFT), and plot the input and the recovered pulses in time domain in Fig. 4. The recovered pulses of Gaus-

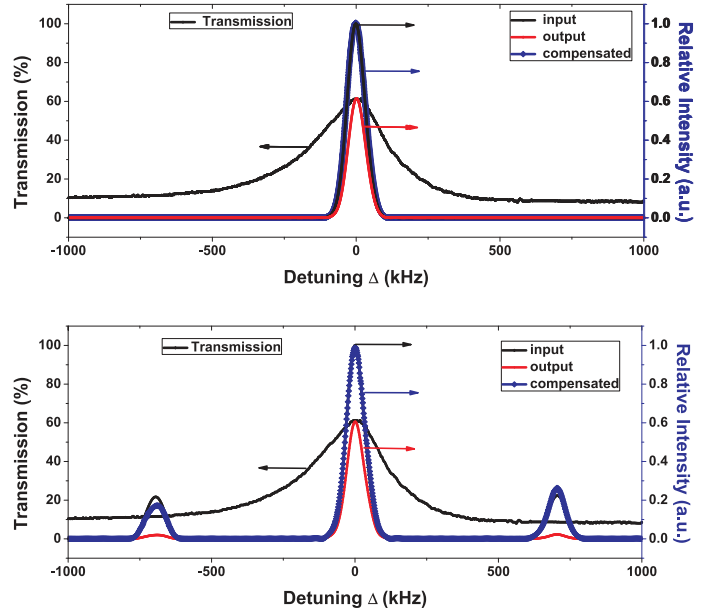


Fig. 3. (color online). The intensity spectrums of input (black solid), output (red solid) and compensated (blue solid with bar) pulses, and the transmission spectrum. (a) Gaussian case. The compensated spectrum overlaps with the input one. (b) AMG case. The compensated spectrum overlaps with the corresponding input one only with minor deviations.

sian and AMG, with different time delays, are both in good agreement with their corresponding input pulses in shape and intensity. Especially in the AMG case, even with the significant loss and distortion, both the intensity and the shape of the slowed pulse are well recovered.

The different spectral components, according to $\Phi(\Delta)$, also experience different phase shift, which leads to dispersion and introduces a certain distortion that is not severe in our case. By separately transforming each spectral component back to time domain using IDFT, we obtain three Gaussian pulses with absolutely different “time-delays”. For the resonant component, we obtain the “slow light” of a Gaussian pulse [$\sim 0.47 \mu\text{s}$, see Fig. 5] with an identical time delay with the non-modulated Gaussian one [$\sim 0.47 \mu\text{s}$, see Fig. 4(a)]. On the contrary, for each sideband (left or right) component, we obtain a Gaussian pulse even with a little time advancing [$\sim 0.18 \mu\text{s}$ or $\sim 0.20 \mu\text{s}$, see Fig. 5], namely “fast light”. It should be pointed out that this phenomenon, called “simultaneous slow and fast light”, is of different spectral components of a single pulse while that presented in [14] is of different polarized pulses. The intensities of left and right sideband spectral components (fast light) in Fig. 5 have a minor difference, since they experience different absorptions due to the asymmetry of energy level structure. As a result, the time delay of slowed AMG pulse is decreased since it is a result of the interfering superposition of the three separate spectral components which tells why the Gaussian and AMG pulses experience dif-

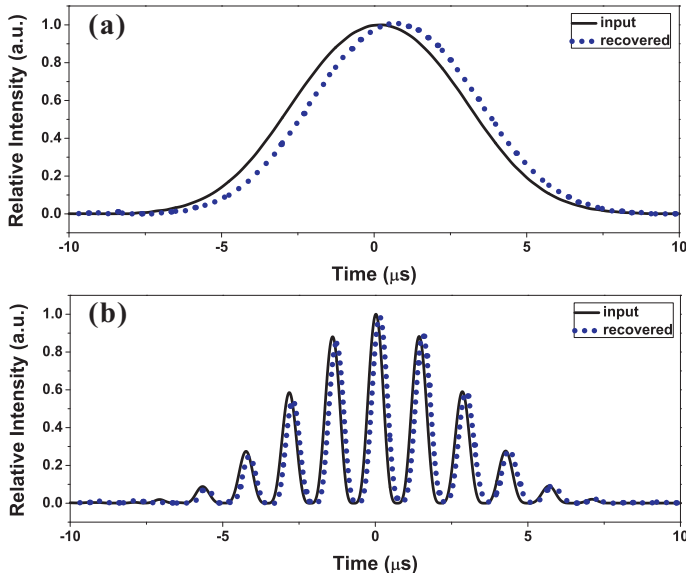


Fig. 4. (color online). Input and recovered (calculated from the compensated spectrum in Fig. 3) pulses in time domain. (a) Gaussian case. Delay time $\sim 0.46 \mu\text{s}$ is measured according to the peak of pulse. (b) AMG case. Delay time $\sim 0.11 \mu\text{s}$ is measured according to the highest peak of pulse.

ferent time-delays [see Fig. 2].

On the other hand, this “simultaneous slow and fast light” effect in a single pulse will inevitably cause an additional pulse distortion (“dispersive distortion”), but here it is negligibly small for such a single- Λ type system [15, 16]. Actually, a good compensating result has been obtained without eliminating the dispersive distortion. However, if the dispersive distortion is so severe that a single AMG pulse splits into two or three pulses, the compensation method we proposed is no longer valid.

In addition, the delay time of the Gaussian pulse [$\sim 0.47 \mu\text{s}$, see Fig. 2(a)] remains approximately unchanged after compensation [$\sim 0.46 \mu\text{s}$, see Fig. 4(a)], because its spectrum has relatively intensive distribution within the transparency window. By contrast, the delay time of the recovered AMG pulse [$\sim 0.11 \mu\text{s}$, see Fig. 4(b)] is decreased during the compensating process [compared with the delay $\sim 0.14 \mu\text{s}$ of the output pulse in Fig. 2(b)]. That is to say, to a certain extent, the compensation method weakens the slow light effect of the AMG pulse. This is because that, these separate spectral components propagating with definitely different group velocities (i.e., “slow and fast light”), are amplified by different magnitudes during the compensating process. The fast light effect of the two sideband components are enhanced larger than the slow light effect of the resonant one, so that the delay time of the recovered AMG pulse, as an interfering superposition of three spectral components, is undoubtedly reduced. Therefore, when applying this compensation, we should make a trade-off between the pulse shape

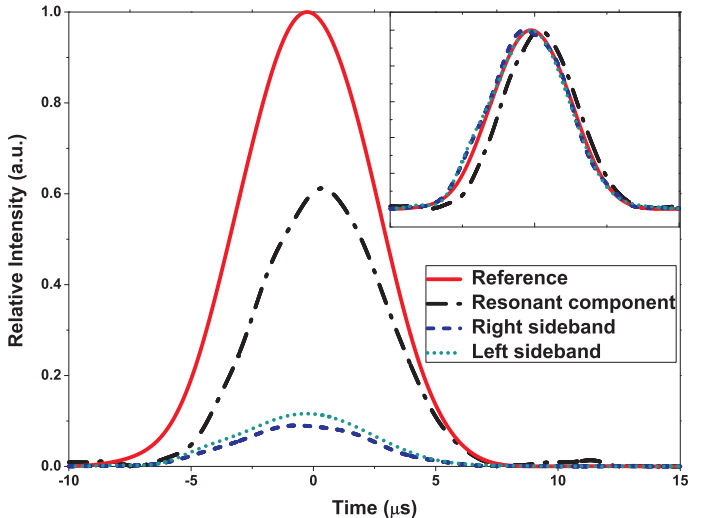


Fig. 5. (color online). Simultaneous slow and fast light of the separate spectral components of a single AMG pulse. Using IDFT, the resonant and two sideband components (left and right) are obtained from the corresponding spectral components of the output AMG pulse [Fig. 3(b)], while a common reference pulse is obtained from any (resonant, left or right) spectral component of the input AMG pulse. As a result, the resonant spectral component propagates as slow light, while both left and right sideband ones propagate as fast light. The delayed (advanced) time $\sim 0.47 \mu\text{s}$ ($\sim 0.18 \mu\text{s}$ for left, $\sim 0.20 \mu\text{s}$ for right) is measured according to the peak of pulse. In the inset, all the pulses are normalized for comparison.

(intensity) and time delay, i.e., to determine whether it is worth while to compensate the loss and distortion with such a reduction of time delay.

4. DISCUSSION AND CONCLUSION

In conclusion, according to our knowledge, the slow light of a single amplitude-modulated pulse is studied for the first time. We present a post-processing method for pulse recovering in slow light. Taking the cosine-type AMG pulse as an example, we focus on the study on the pulse distortion (loss) and compensation in a single- Λ EIT system, which is distinguished from that attempting to optimize the pulse shape with large delay and small broadening in Brillouin fiber slow-light systems [17]. We experimentally demonstrate that both the loss and distortion of the amplitude modulated pulse are significant. Then we analyze them in frequency domain, and point out that the distortion is mainly caused by different transmission rates for different spectral components. Accordingly, we present a compensation method to recover the shape and intensity of the slowed pulse with high fidelity. Further, in our system, the dispersion effect will inevitably cause, additionally, small distortion for the AMG pulse. More importantly, this effect reveals a novel way, different from [14], to realize simultaneous slow and fast light of different spectral components in a single optical

pulse. Because the compensating process will always affect the time delay of an AMG pulse, a trade-off between pulse shape (intensity) and time delay should be made in applications. In principle, all the aforementioned results can be extended to an arbitrary amplitude modulated pulse in a single- Λ type EIT system. It is reasonable to believe that these methods of amplitude modulation and recovering of a single pulse in slow light would have potential applications in optical communication and low-distortion optical delay lines.

ACKNOWLEDGEMENT

This work is supported by the Key Project of the National Natural Science Foundation of China (Grant No. 60837004), and the Open Fund of Key Laboratory of Optical Communication and Lightwave Technologies (Beijing University of Posts and Telecommunications), Ministry of Education, P. R. China.

References

1. S. E. Harris, "Electromagnetically Induced Transparency," *Phys. Today* **50**, 36-42 (1997).
2. M. Fleischhauer, A. Imamoglu, and J. P. Marangos, "Electromagnetically induced transparency: Optics in coherent media," *Rev. Mod. Phys.* **77**, 633-673 (2005).
3. R. M. Camacho, M. V. Pack, J. C. Howell, A. Schweinsberg, and R. W. Boyd, "Wide-Bandwidth, Tunable, Multiple-Pulse-Width Optical Delays Using Slow Light in Cesium Vapor," *Phys. Rev. Lett.* **98**, 153601 (2007).
4. R. M. Camacho, C. J. Broadbent, I. Ali-Khan, and J. C. Howell, "All-Optical Delay of Images using Slow Light," *Phys. Rev. Lett.* **98**, 043902 (2007).
5. S. W. Chang, S. L. Chuang, P.-C. Ku, C. J. Chang-Hasnain, P. Palinginis, and H. Wang, "Slow light using excitonic population oscillation," *Phys. Rev. B* **70**, 235333 (2004).
6. P. Palinginis, F. Sedgwick, S. Crankshaw, M. Moewe, and C. J. Chang-Hasnain, "Room temperature slow light in a quantum-well waveguide via coherent population oscillation," *Opt. Express* **13**, 9909-9915 (2005).
7. Y. Okawachi, M. S. Bigelow, J. E. Sharping, Z. Zhu, A. Schweinsberg, D. J. Gauthier, R. W. Boyd, and A. L. Gaeta, "Tunable All-Optical Delays via Brillouin Slow Light in an Optical Fiber," *Phys. Rev. Lett.* **94**, 153902 (2005).
8. J. E. Sharping, Y. Okawachi, and A. L. Gaeta, "Wide bandwidth slow light using a Raman fiber amplifier," *Opt. Express* **13**, 6092-6098 (2005).
9. A. B. Matsko, D. V. Strekalov, and L. Maleki, "On the dynamic range of optical delay lines based on coherent atomic media," *Opt. Express* **13**, 2210-2223 (2005).
10. M. D. Stenner, D. J. Gauthier, and M. A. Neifeld, "Fast causal information transmission in a medium with a slow group velocity," *Phys. Rev. Lett.* **94**, 053902 (2005).
11. J. Gea-Banacloche, Y. Li, S. Jin, and M. Xiao, "Electromagnetically induced transparency in ladder-type inhomogeneously broadened media: Theory and experiment," *Phys. Rev. A* **51**, 576-584 (1995).
12. M. D. Stenner, M. A. Neifeld, Z. Zhu, A. M. Dawes, and D. J. Gauthier, "Distortion management in slow-light pulse delay," *Opt. Express* **13**, 9995-10002 (2005).
13. G. Nikoghosyan and G. Grigoryan, "Influence of relaxation on propagation, storage, and retrieving of light pulses in a medium with electromagnetically induced transparency," *Phys. Rev. A* **72**, 043814 (2005).
14. J. Zhang, G. Hernandez, and Y. Zhu, "Copropagating superluminal and slow light manifested by electromagnetically assisted nonlinear optical processes," *Opt. Lett.* **31**, 2598-2600 (2006).
15. R. W. Boyd, D. J. Gauthier, A. L. Gaeta, and A. E. Wilner, "Maximum time delay achievable on propagation through a slow-light medium," *Phys. Rev. A* **71**, 023801 (2005).
16. R. M. Camacho, M. V. Pack, and J. C. Howell, "Low-distortion slow light using two absorption resonances," *Phys. Rev. A* **73**, 063812 (2006).
17. S. Chin and L. Thevenaz, "Optimized shaping of isolated pulses in Brillouin fiber slow-light systems," *Opt. Lett.* **34**, 707-709 (2009).